SCREENING OF ASHITABA (*ANGELICA KEISKEI* K.) COMPOUNDS AS POTENTIAL *MYCOBACTERIUM TUBERCULOSIS* KASA INHIBITORS

AIYI ASNAWI[1]*, ELLIN FEBRINA[2], WIDHYA ALIGITA[1], DEWI KURNIA[1], LA ODE AMAN[3], ANNE YULIANTINI[1]

[1]Department of Pharmacochemistry, Faculty of Pharmacy, Universitas Bhakti Kencana, Jl. Soekarno-Hatta No. 754, Bandung, 40617, Indonesia, [2]Department of Pharmacology and Clinical Pharmacy, Faculty of Pharmacy, Universitas Padjadjaran, Jl. Raya Bandung-Sumedang Km. 21, Jatinangor, 45363, Indonesia, [3]Department of Chemistry, Faculty of Mathematics and Natural Science, Universitas Negeri Gorontalo Jl. Jend. Sudirman No. 6 Kota Gorontalo, Gorontalo, 96128, Indonesia
*Email: aiyi.asnawi@bku.ac.id

ABSTRACT

Objective: Tuberculosis (TB) is a major global issue, mainly owing to the emergence of antibiotic-resistant strains of the disease's causative agent, *Mycobacterium tuberculosis*. The current standard of treatment for tuberculosis entails a prolonged course of antibiotics with toxic side effects and is accompanied by low patient compliance. Therefore, developing and discovering TB medications is critical to obtaining TB drugs that are more effective and sensitive to *Mycobacterium tuberculosis*. Ashitaba (*Angelica keiskei* K.) has reported that Ashitaba extract and chalcone have anti-TB properties, but the responsible compound has not been reported yet. This study aimed to identify the profile metabolites present in Ashitaba and their interaction with *Mycobacterium tuberculosis* KasA.

Methods: To suggest these, we used molecular docking and molecular dynamic to predict the interactions of 40 selected compounds from the Ashitaba against *Mycobacterium tuberculosis* KasA (PDB ID 2WGE).

Results: The results of molecular docking identified the top two compounds as xanthoangelol I (XAI) and (2E)-1-[4-hydroxy-2-(2-hydroxy-2-propanyl)-2,3-dihydro-1-benzofuran-7-yl]-3-(4-hydroxyphenyl)-2-propen-1-one (4HH), with bond free energies of-12.03 and-11.87 kcal/mol, respectively. Based on the results of molecular dynamics simulations, the XAI was stronger than 4HH in stabilizing complexes with 2WGE with total energy (ΔGbind, MMGBSA) of-54.8512 and-37.8836 kcal/mol, respectively.

Conclusion: It can be concluded that xanthoangelol I (XAI) have the most potent inhibitor of Mycobacterium tuberculosis KasA.

Keywords: Ashitaba, *In silico*, KasA, *Mycobacterium tuberculosis*, Molecular docking, Molecular dynamics

INTRODUCTION

Tuberculosis (TB) is the most significant infectious disease cause of death, with 10 million new cases in 2017. It is estimated that over 1.7 billion people have latent tuberculosis infection and are at risk of developing active TB disease during their lifetime [1]. The rise of multidrug-resistant (MDR) and extremely drug-resistant (XDR) tuberculosis is primarily attributable to the inappropriate administration of first-line antitubercular medication. The rising incidence of these strains has become a significant barrier to treating tuberculosis and a considerable cost burden on the healthcare industry. Because of this, there is an urgent need for new, cheap anti-TB drugs that work in new ways and have a lower risk of drug resistance [2].

Mycobacteria have a unique cell wall composed of mycolic acid, a lipid with an extremely long chain that provides protection and enables the bacteria to live in human macrophages. *Mycobacterium tuberculosis* is killed by inhibiting cell wall production. This served as the impetus for the discovery and development of new anti-TB medications. Two distinct beta-ketoacyl synthases (kasA and kasB) are involved in isoniazid sensitivity and mycolic acid production in Mycobacterium TB. KasA, mycobacterial β-ketoacyl ACP synthase I, is a crucial FAS-II system enzyme. FAS-II enzyme inhibitors, with isoniazid as a first-line antibiotic targeting InhA to compromise cell wall integrity.

Mycobacteria have a unique cell wall consisting of mycolic acid, a very long chain lipid that provides protection and allows the bacteria to survive in human macrophages. Inhibition of cell wall biosynthesis is fatal for *Mycobacterium tuberculosis* [3]. This became the starting point for the discovery and development of new anti-TB drugs. *Mycobacterium tuberculosis* has two discrete beta-ketoacyl synthases (KasA and KasB), which are involved in isoniazid sensitivity and mycolic acid synthesis. KasA, mycobacterial β-ketoacyl ACP synthase I, is an important key enzyme in the FAS-II system. FAS-II enzyme inhibitors, with isoniazid, a first-line antibiotic targeting InhA, would impair cell wall integrity [4].

Medicinal plants are a vital biological resource for traditional medical systems. In addition, with the development of phytochemical techniques, numerous active components of medicinal plants have been identified and have begun to be utilized as medications in contemporary medical systems. Ashitaba (*Angelica keiskei* K.) has been utilized as traditional medicine and some research has reported that the Ashitaba extract and its chalcone have anti-TB properties [5] and that chalcone has an anti-TB impact [6], but the responsible compound has not been reported yet.

In drug discovery, computational techniques like molecular docking and molecular dynamics (MD) are influence used to mimic atomic-level interactions between a small molecule (ligand) and a known macromolecule [7]. The overall drug development process can be sped up by using computational approaches in drug discovery to screen candidate compounds before *in vitro* cell culture-based assays or chemical kits [8]. The recent application of molecular docking and MD techniques to identify the lead compound from medicinal plants has shown the technique's importance [9, 10]. Therefore, this paper aimed to use computational techniques to identify the responsible phytochemicals from Ashitaba (*Angelica keiskei* K.) in inhibiting the *Mycobacterium tuberculosis* KasA. We predict the binding of phytochemicals from Ashitaba (*Angelica keiskei* K.) about the control, a proven inhibitor of the molecular target of *Mycobacterium tuberculosis* KasA (PDB ID 2WGE). We also show that ligands with considerably higher docking scores have a superior stable interaction in complexes with the *Mycobacterium tuberculosis* KasA (PDB ID 2WGE) protein crystal structure. The potent lead compound's potency should make *in vitro* investigations easier.

MATERIALS AND METHODS

Materials

The personal computer was equipped with an Intel® Core™ i7-7200U CPU @2.50 GHz (4 CPUs. 2.7 GHz), 20 GB of RAM, and two

operating systems: Linux Ubuntu 18.04 64-bit and Windows 10 Pro-64-bit for molecular docking and MD simulation. The three-dimensional structures of Ashitaba (*Angelica keiskei* K.) compounds were retrieved from the NCBI PubChem Compound database [11]. *Mycobacterium tuberculosis* KasA [12], which had a PDB code of 2WGE, was the model of the protein's three-dimensional structure obtained from the website of protein databank (http://www. rscb. org/pdb). With the ability to rotate in both Discovery Studio Visualizer and AutoDockTools-1.5.6, polar hydrogen atoms were added to the structure of the ligand.

Molecular docking simulation

The proteins *Mycobacterium Tuberculosis* KasA and ligands were docked using the AutoDock 4.2 Release 4.2.6 program [13]. The molecular docking simulation was performed in the following order (for more details, see Febrina *et al.*, 2021) [14]: The protein and the ligands both have polar hydrogen and Kollman charges we introduced into them. The ligand coordinates were flexible and migrated about the grid map built around TLM as the native ligand, while the protein coordinates stayed fixed. The centre of the grid box was determined by the docking procedure validation and using that information, the sizes (52, 42, and 40) and centres (37.883, 1.178, and-6.411) of the grid box, as well as the spacing, have been set to 0.375 Å were determined and employed. The validation of the docking process was utilized to determine the centre of the grid box, and the test compounds (ligands) were designed based on this information. A Gasteiger charge was added to each ligand atom to produce the ligand. A Lamarckian genetic algorithm (LGA) was utilized to discover the optimal docking conformations, and each ligand performed a total of 150 independent runs. There was a maximum of 150 placed on the overall number of participants. The total number of generation accounts for 27 000, while the total number of energy evaluations amounts to 2 500 000. The discovery studio visualizer was then used to depict the binding interaction as well as the processes that were associated with it.

Molecular dynamics simulation

All MD simulations were carried out using the AMBER18 program. The docking best poses were used to generate the starting structure for MD simulations of 2WGE complexes with TLM, XAI, or 4HH. A software database was used to add the FF14SB force field and charge to the protein. Due to the ligand's absence of partial charge parameters in the GAFF force field, a generalized force field (GAFF2) was applied to them, and the AM1-BCC method was used to quantify their partial charge. The AMBER18 package includes the Antechamber suite, which was used to generate topology files and ligand atomic payloads. AMBER18's Tleap module was used to build the system's topology and coordinate files. With a margin of 10 Å, the entire system was immersed in a box containing TIP3P water solvent. Some sodium ions (Na$^+$) were introduced to neutralize the

system's charge. During the MD simulation, an Ewald particle mesh (PME) was used to address long-range electrostatic interactions, and the non-bonded interaction distance was set to 10 Å. The SHAKE algorithm restricts hydrogen-based bonds.

The MD simulation was performed in the following order (for more details, see Asnawi *et al.*, 2022) [9, 14]: First, each system underwent three stages of energy minimization utilizing the 1000-step steepest descent and 1000-step conjugate gradient algorithms. Using the same method, this was accomplished through protein restraint in the first and second stages and without any restrictions in the third stage. Secondly, each system was heated in 20 picoseconds (ps) increments from 0 to 310 K. The system was then balanced to 100 psi at 310 K with constant pressure. The production process was completed in the final stage for 50-150 ns (different for each complex), at constant temperature and pressure (NTP), with a step of 1 fs. The RMSD chart recorded movements every ten ps, and protein fluctuations were evaluated using RMSF. The MM/GBSA approach was used to quantify the receptor-ligand complex's relative binding free energy ($\otimes G_{bind}$). In the final one ns pass of the MD simulation, all portraits of the simulated structures were extracted for computation.

RESULTS

Validation of docking protocol

The docking procedure was validated using the Lamarckian Genetic Algorithm approach, with the number of runs set to 100 and the number of evals set to Medium. Grid points are 52, 42, and 40 in size, with grid centre coordinates of 37.883, 1.178, and 6.411. Fig. 1 depicts the visualization of TLM overlays from redocking with co-crystal ligands from crystallographic data. Finally, the redocking procedure demonstrates that the docking protocol may be used for docking.
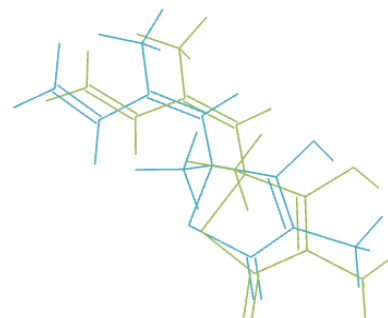

Fig. 1: Overlays of TLM (native ligand) from the redocking result (blue) with co-crystal of TLM from X-crystallography data (green) at receptors 2WGE with RMSD of 0.486 Å

Table 1: Docking score of the ligands in the active site of KasA (PDB ID 2WGE)

No.	Compounds name	Code	Estimated free energy of binding (ΔG), (kcal/mol)	Estimated inhibition constant (Ki), µM
	Thiolactomycin	TLM	-8.64	0.46279
1	(3′r)-3′-hydroxy-columbianidin	3HC	-10.03	0.04430
2	3′-senecioyl khellactone	3SK	-8.61	0.48626
3	4-hydroxyderricin	4HD	-9.65	0.08419
4	(2e)-1-[4-hydroxy-2-(2-hydroxy-2-propanyl)-2,3-dihydro-1-benzofuran-7-yl]-3-(4-hydroxyphenyl)-2-propen-1-one	4HH*	-11.87	0.00198
5	(2e)-1-[4-hydroxy-2-(2-hydroxy-6-methyl-5-hepten-2-yl)-2,3-dihydro-1-benzofuran-5-yl]-3-(4-hydroxyphenyl)-2-propen-1-one	4HM	-10.39	0.02429
6	4-hydroxy-3,5,5-trimethyl-4-(1,2,3,-trihydroxybutyl)cyclohex-2-enone	4HT	-6.40	20.20
7	(2E)-1-(3-[(2E)-6-hydroperoxy-3,7-dimethyl-2,7-octadien-1-yl]-2-hydroxy-4-methoxyphenyl)-3-(4-hydroxyphenyl)-2-propen-1-one	4OG	-11.38	0.00457
8	4′-senecioyl khellactone	4SK	-9.47	0.11444
9	5-methoxyprosalen	5MP	-7.20	5.31
10	(2e)-1-(3-[(2e)-6,7-dihydroxy-3,7-dimethyl-2-octen-1-yl]-2,4-dihydroxy phenyl)-3-(4-hydroxyphenyl)-2-propen-1-one	6DD	-10.23	0.03189
11	8-Geranylnaringenin	8GN	-11.00	0.00861
12	Archangelicin	ARC	-11.12	0.00707

| No.	Compounds name	Code	Estimated free energy of binding (ΔG), (kcal/mol)	Estimated inhibition constant (Ki), µM
13	Ashitabaol A	AS_A	-8.30	0.82523
14	Demethylsuberosin	DMS	-8.18	1.01
15	Falcarindiol	FCR	-7.65	2.48
16	Isobavachin	IBVN	-10.74	0.01346
17	Isobavachalcone	ISC	-10.44	0.02236
18	Isolaserpitin	ISP	-9.85	0.06022
19	Laserpitin	LSP	-6.47	18.02
20	Munduleaflavanone	MFN	-9.84	0.06080
21	Munduleaflavanone B	MFN_B	-10.73	0.01369
22	Osthenol	OSN	-8.03	1.30
23	Prostratol F	PRF*	-11.16	6.65
24	Pregnenolone	PRG	-8.67	0.44213
25	Pteryxin	PTX	-9.38	0.13248
26	Selinidin	SLD	-8.86	0.31923
27	Xanthoangelol	XA	-10.22	0.03216
28	Xanthoangelol B	XA_B	-10.21	0.03282
29	Xanthoangelol C	XA_C	-9.71	0.07664
30	Xanthoangelol D	XA_D	-9.88	0.05698
31	Xanthoangelol E	XA_E	-10.61	0.01666
32	Xanthoangelol F	XA_F	-10.34	0.02656
33	Xanthoangelol G	XA_G	-9.08	0.22086
34	Xanthoangelol H	XA_H	-11.46	0.00398
35	Xanthokeismin A	XAA	-10.16	0.03580
36	Xanthokeismin B	XAB	-10.60	0.01703
37	Xanthokeismin C	XAC	-10.11	0.03914
38	Xanthoangelol I	XAI*	-12.03	0.00152
39	Xanthoangelol J	XAJ	-10.67	0.01509
40	Xanthoangelol K	XAK	-9.76	0.07047
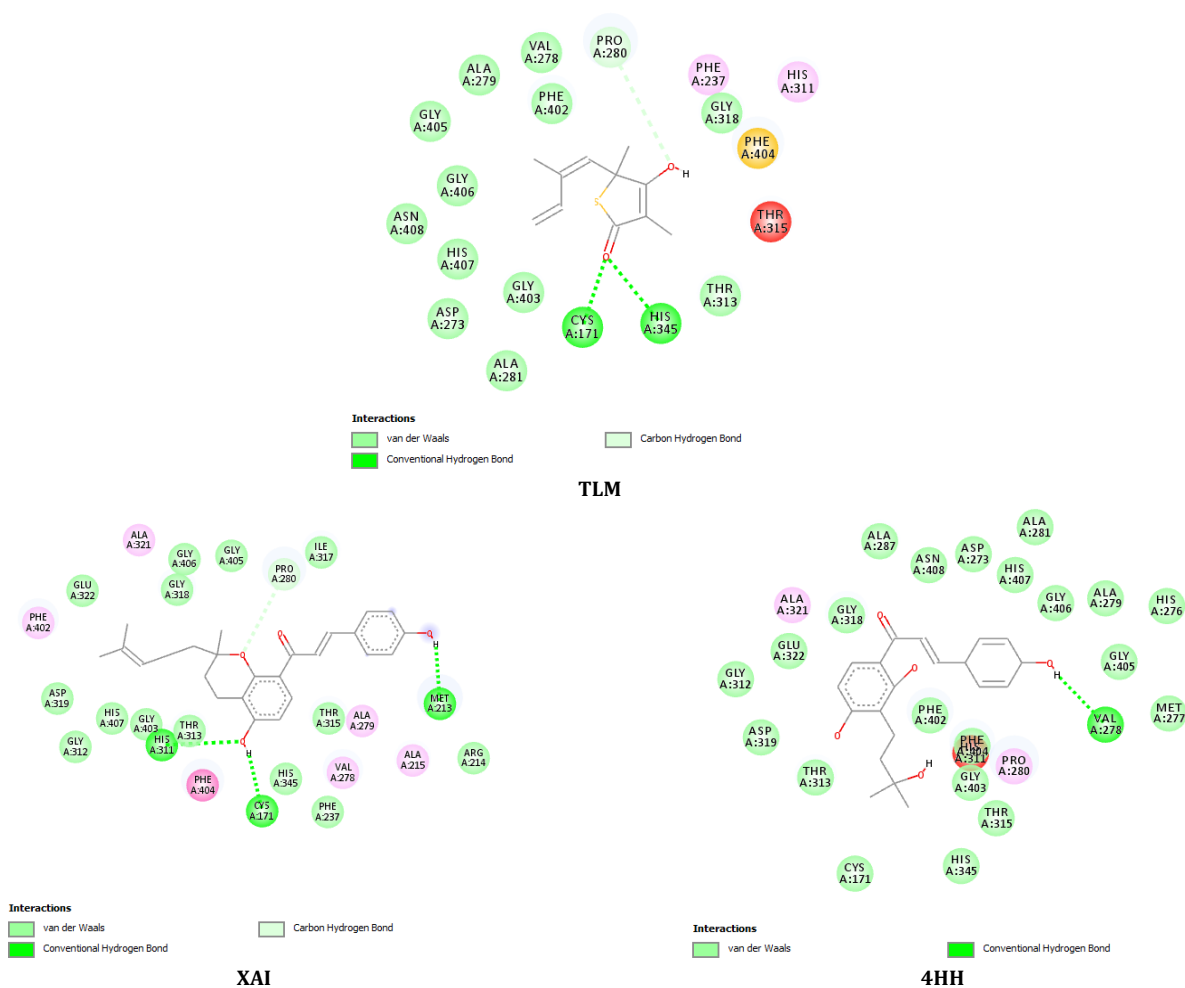
Fig. 2: 2D interactions of native ligan (TLM), 4HH, and XAI in 2WGE receptor amino acid residues

In silico screening analysis

In silico screening of 40 test ligands (from various sources paper) at the 2WGE receptor showed that 23 compounds had more negative energy than native ligand (TLM) as well as the drug molecule, GSK724 [15] (a positive control), in terms of binding free energy and inhibition constants (table 1 and fig. 3). These have mechanisms such as Kas-A inhibitors (2WGE) [16].

Molecular dynamics analysis

RMSD

The docking best poses were used to study how solvents and the flexibility of proteins affect how receptors and ligands interact. To assess the simulation's stability, the parameters of each complex, such as temperature, pressure, energy, and structure, were evaluated along the MD trajectory (fig. 3).
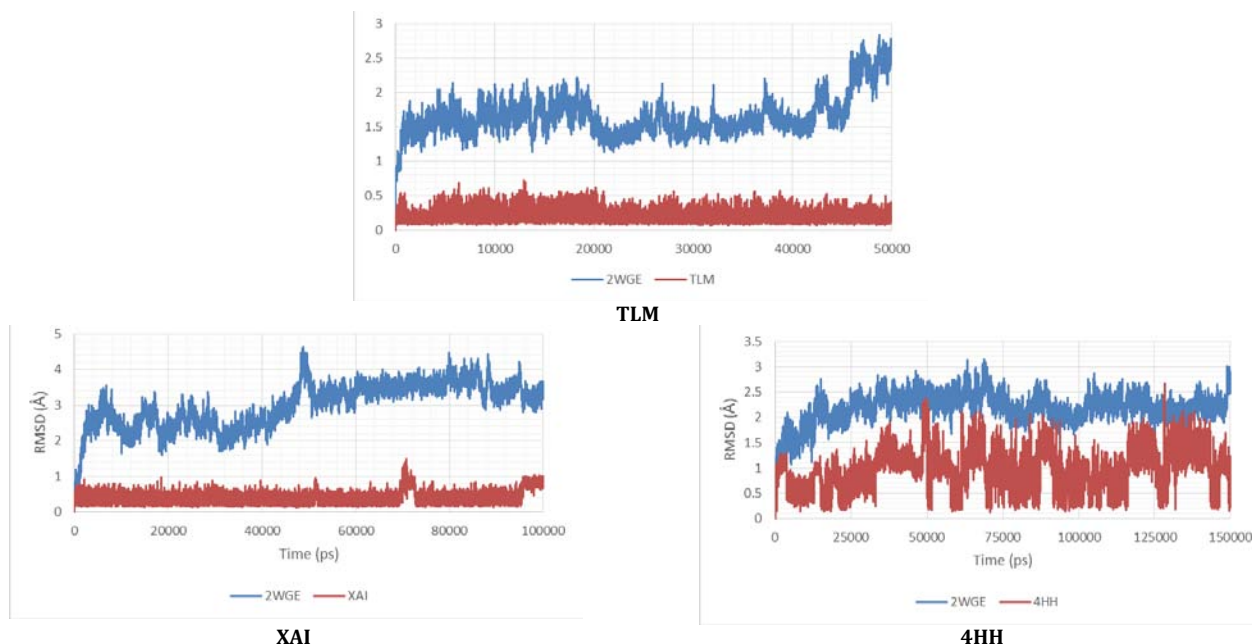

TLM

XAI

4HH

Fig. 3: The root mean squared deviation (RMSD) of 2WGE backbone (blue) and ligand (red)

RMSF

RMSF was employed in MD simulations to evaluate the stability of residues in the binding pocket. The RMSF of each residue near the ligand was determined using the data of the last one ns of the trajectory (fig. 4).

MMGBSA (Energy component estimation)

The MMGBSA study determines the free energy required to bind macromolecules and ligands by combining molecular mechanics calculations and continuum solvation models (table 2).
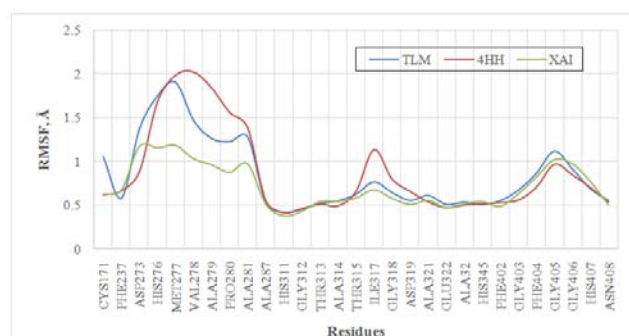

Fig. 4: The root mean squared fluctuation (RMSF) of resiues at 2WGE backbone

Table 2: Energy component of the ligands into in the pocket of 2WGE

Energy component	2WGE–TLM (kcal/mol)	2WGE–4HH (kcal/mol)	2WGE–XAI (kcal/mol)
ΔE_{vdw}	-35.1535	-40.5253	-58.7883
ΔE_{ele}	-12.3372	-30.3353	-18.9273
ΔE_{gas}	-47.4907	-70.8606	-77.7157
ΔG_{GB}	20.5443	38.7816	30.1072
ΔG_{SA}	-4.1777	-5.8047	-7.2427
ΔG_{sol}	16.3666	32.9770	22.8644
ΔG_{bind}	-31.1241	-37.8836	-54.8512

Description: ΔE_{vdw}: van der Waals potential energy; ΔE_{ele}: electrostatic energy; ΔE_{gas}: mechanical molecular energy in the gas phase; ΔG_{GB}: polar solvation-free energy; ΔG_{SA}: non-polar solvation free energy; ΔG_{sol}: solvation-free energy; ΔG_{bind}: bond free energy.

DISCUSSION

Molecular docking

The RMSD (Root-Mean-Square Deviation) of atomic positions for TLM derived from these parameters on docking procedure validation for the 2WGE receptor was 0.486 Å. This RMSD indicated that the docking methodology was suitable for docking. The top three ligands with the lowest binding free energies were XAI, 4HH, and PRF. These ligands had values of 12.03,-11.87, and-11.16 kcal/mol, respectively. After researching and contrasting the ligand's binding free energies and inhibition constants, we determined that XAI and 4HH were the most effective candidates for the pose ligand role. It was because the inhibition constants of the PRF ligand were more significant than those of the other two ligands. Based on this feature, it would appear that XAI interacts more favourably than the pharmaceutical molecule GSK724. Even though the 4HH does not interact as effectively as GSK724, its potential shows excellent promise.

There might be variations in the binding between each test evaluation and amino acids and the type of binding that occurs due to differences in the affinity between test compounds and receptors (table 1 and fig.). The results demonstrated that ligands form bonds with various amino acids. The XAI has three hydrogen bonds, like the hydrogen interactions seen in native ligand, 11 hydrophobic interactions, and nine vans der Waals interactions, according to an analysis of the interactions of compounds targeting 2WGE. 4HH possesses one unbonded hydrogen bond with amino acid residues analogous to the native ligand, three hydrophobic interactions, and sixteen vans der Waals contacts. The hydrophobic and van der Waals interactions contribute to more negative binding energy in 4HH (Table-1). The TLM interacts with Cys171, Pro280, and His345 by forming hydrogen bonds and with Phe237, Pro280, His311, and Phe404 through the formation of hydrophobic bonds. The 4HH interacts with Val278 by a hydrogen bond and with Pro280 and His311 through hydrophobic interactions. The XAI interacts with other molecules by forming hydrogen bonds with Pro280, Cys171, and His311; and hydrophobic bonds with Val278, Aal279, Pro280, His311, Phe402, and Phe404. The order of the most potent compounds determined that XAI and 4HH had the best negative energy among other compounds. It is critical to investigate how these two ligands interact to stabilize complexes with the 2WGE receptor.

Molecular dynamics analysis

An investigation into how these two ligands, XAI and 4HH, interact to stabilize complexes with the 2WGE receptor was carried out with the help of an MD simulation. The outcomes of an MD simulation include the root-mean-square deviation (RMSD) of atomic positions, the root-mean-square-fluctuation (RMSF) of a structure, and the MM/GBSA ΔG bind and its energy components.

RMSD

It takes the 2WGE-TLM complex precisely one nanosecond to reach equilibrium, and its average RMSD fluctuations for protein and ligands are 1.65 and 0.20 Å, respectively. The average RMSD fluctuations for protein and ligands in the 2WGE-XAI complex were 2.99 and 0.39 Å, respectively, and the complex reached equilibrium after one ns of time. On the other hand, the average RMSD fluctuations for protein and ligands in the 2WGE-4HH complex were 2.18 and 0.95 Å, respectively, and the complex reached equilibrium at ten to 40 ns. However, this complex started to experience significant fluctuations at 50 ns with RMSD>2Å. This fluctuation most probably caused the change in the interaction pattern between the 4HH ligand and the 2WGE residues. If the simulation's initial best position did not allow 4HH to bind to the residue stably, the simulation could show this. Comparing the results of RMSD to TLM and 4HH showed that XAI was the compound that could stabilize the complex the most (fig. 3).

RMSF

In three distinct locations (the Cys171-Ala287 region, the Thr315-Asp319 part, and the Phe402-Asn408 region), all selected complexes exhibited fluctuation patterns of residues that were generally comparable to one another. It is plausible to conclude that the residue was still in the stable category for these two locations if the three complexes exhibited changes less than 2 Å, which occurred in each of the most recent locations. On the other hand, in the first area, the fluctuation of residues for the TLM-2WGE and 4HH-2WGE complexes is rather substantial, with the RMSF reaching 1.9085 and 2.0197 Å, respectively. It was indicated that these complexes have a high degree of structural disorder. It can be deduced from this that these complexes have significant structural disarray. However, the XAI-2WGE complex had an average fluctuation of less than 1.2 Å. Both the results obtained from the RMSD analysis and the results obtained from the RMSF research (fig. 4) were similar to one another, indicating that they are consistent with one another (fig. 3).

MMGBSA (Energy component estimation)

The 2WGE-XAI complex was more stable than the 2WGE-TLM complex and the 2WGE-4HH complex, which each had values of-31.1241 and-37.8836 kcal/mol for their bond-free energies, respectively. The 2WGE-XAI complex had bond-free energies of-54.8512 kcal/mol (table 2).

It has been demonstrated that the docking energy is compatible with these findings (table 1). Nevertheless, the stability of the 2WGE-XAI complex can be affected by the van der Waals interaction, the mechanical molecular energy in the gas phase, and the non-polar solvation-free energy. In addition to being affected by electrostatic energy, polar solvation-free energy, and solvation-free energy, the 2WGE-4HH complex is also impacted by additional types of free energy.

CONCLUSION

Both XAI (xanthoangelol I) and 4HH ((2E)-1-[4-hydroxy-2-(2-hydroxy-2-propanyl)-2,3-dihydro-1-benzofuran-7-yl]-3-(4-hydroxyphenyl)-2-propen-1-one), exhibit more negative binding energies than native ligand when they bind to the 2WGE protein. In contrast, xanthoangelol I have a larger capacity to stabilize complexes by MMGBSA adversely. It shows that xanthoangelol I could act as a lead compound in *Mycobacterium Tuberculosis* KasA.

AUTHORS CONTRIBUTIONS

Every single one of the writers has made a significant contribution to the current study.

CONFLICT OF INTERESTS

The authors state that there are no competing interests involved.

REFERENCES

1. Floyd K, Glaziou P, Zumla A, Raviglione M. The global tuberculosis epidemic and progress in care, prevention, and research: an overview in year 3 of the End TB era. Lancet Respir Med. 2018 Apr 1;6(4):299-314. doi: 10.1016/S2213-2600(18)30057-2, PMID 29595511.
2. Baptista R, Bhowmick S, Nash RJ, Baillie L, Mur LAJ. Target discovery-focused approaches to overcome bottlenecks in the exploitation of antimycobacterial natural products. Future Med Chem. 2018 Apr 1;10(7):811-22. doi: 10.4155/fmc-2017-0273, PMID 29569936.
3. Slayden RA, Barry CE. The role of KasA and KasB in the biosynthesis of meromycolic acids and isoniazid resistance in Mycobacterium tuberculosis. Tuberculosis (Edinb). 2002;82(4-5):149-60. doi: 10.1054/tube.2002.0333, PMID 12464486.
4. Slayden RA, Lee RE, Armour JW, Cooper AM, Orme IM, Brennan PJ. Antimycobacterial action of thiolactomycin: an inhibitor of fatty acid and mycolic acid synthesis. Antimicrob Agents

Chemother. 1996;40(12):2813-9. doi: 10.1128/AAC.40.12.2813, PMID 9124847.

5. Kusuma SAF, Iskandar Y, Dewanti MA. The ethanolic extract of ashitaba stem (Angelica keskei [Miq.] Koidz) as future antituberculosis. J Adv Pharm Technol Res. 2018;9(1):37-41. doi: 10.4103/japtr.JAPTR_283_17, PMID 29441323.

6. Lin YM, Zhou Y, Flavin MT, Zhou LM, Nie W, Chen FC. Chalcones and flavonoids as anti-tuberculosis agents. Bioorg Med Chem. 2002;10(8):2795-802. doi: 10.1016/s0968-0896(02)00094-9, PMID 12057669.

7. McConkey BJ, Sobolev V, Edelman M. The performance of current methods in ligand–protein docking. Curr Sci. 2002:845-56.

8. Nursamsiar AA, Kartasasmita RE, Ibrahim S, Tjahjono DH. Synthesis, biological evaluation, and docking analysis of methyl hydroquinone and bromo methyl hydroquinone as potent cyclooxygenase (COX-1 and COX-2) inhibitors. J App Pharm Sci. 2018 Jul 30;8(7):16-20. doi: 10.7324/JAPS.2018.8703/abstract.php?id=2669andsts=2.

9. A Asnawi, Aman LO, Nursamsiar, A Yuliantini, E Febrina. Molecular docking and molecular dynamic studies: screening phytochemicals of Acalypha Indica Against Braf kinase receptors for potential use in melanocytic tumours. Rasayan J Chem. 2022 Apr;15(2):1352-61. doi: 10.31788/RJC.2022.1526769.

10. Nursamsiar, Nur S, Febrina E, Asnawi A, Syafiie S. Synthesis and inhibitory activity of curculigoside A derivatives as potential anti-diabetic agents with β-cell apoptosis. J Mol Struct. 2022;1265:133292. doi: 10.1016/j.molstruc.2022.133292.

11. Li Q, Cheng T, Wang Y, Bryant SH. PubChem as a public resource for drug discovery. Drug Discov Today. 2010 Dec;15(23-24):1052-7. doi: 10.1016/j.drudis.2010.10.003, PMID 20970519.

12. Luckner SR, Machutta CA, Tonge PJ, Kisker C. Crystal structures of Mycobacterium tuberculosis KasA show mode of action within cell wall biosynthesis and its inhibition by thiolactomycin. Structure. 2009 Jul 7;17(7):1004-13. doi: 10.1016/j.str.2009.04.012, PMID 19604480.

13. Bitencourt Ferreira G, Pintro VO, de Azevedo WF. Docking with AutoDock4. Methods Mol Biol. 2019;2053:125-48. doi: 10.1007/978-1-4939-9752-7_9, PMID 31452103.

14. Febrina E, Alamhari RK, Abdulah R, Lestari K, Levita J, Supratman U. Molecular docking and molecular dynamics studies of acalypha Indica L. phytochemical constituents with caspase-3. Int J App Pharm. 2021 Dec 11;13Special Issue 4:210-5. doi: 10.22159/ijap.2021.v13s4.43861.

15. Kumar P, Capodagli GC, Awasthi D, Shrestha R, Maharaja K, Sukheja P. Synergistic lethality of a binary inhibitor of mycobacterium tuberculosis kasA. mBio. 2018 Nov 1;9(6). doi: 10.1128/mBio.02101-17, PMID 30563908.

16. Batt SM, Burke CE, Moorey AR, Besra GS. Antibiotics and resistance: the two-sided coin of the mycobacterial cell wall. Cell Surf. 2020 Dec 1;6:100044. doi: 10.1016/j.tcsw.2020.100044, PMID 32995684.